Monthly Notices of the ROYAL ASTRONOMICAL SOCIETY

MNRAS **514,** L36–L40 (2022) https://doi.org/10.1093/mnrasl/slac055
Advance Access publication 2022 May 17

The twin radio galaxy TRG J104454+354055

Gopal-Krishna,[1] Ravi Joshi [2,3]★ Dusmanta Patra,[4] Xiaolong Yang,[5,6] Luis C. Ho,[3,7] Paul J. Wiita[8] and Amitesh Omar [9]

[1]*UM-DAE Centre for Excellence in Basic Sciences, Mumbai 400098, India*
[2]*Indian Institute of Astrophysics, Koramangla, Bangalore 560034, India*
[3]*Kavli Institute for Astronomy and Astrophysics, Peking University, Beijing 100871, China*
[4]*S N Bose National Centre for Basic Sciences, Kolkata 700106, India*
[5]*Shanghai Astronomical Observatory, Key Laboratory of Radio Astronomy, Chinese Academy of Sciences, Shanghai 200030, China*
[6]*Shanghai Key Laboratory of Space Navigation and Positioning Techniques, Shanghai Astronomical Observatory, Chinese Academy of Sciences, Shanghai 200030, China*
[7]*Department of Astronomy, School of Physics, Peking University, Beijing 100871, China*
[8]*Department of Physics, The College of New Jersey, 2000 Pennington Rd, Ewing, NJ 08628-0718, USA*
[9]*Aryabhatta Research Institute of Observational Sciences, Nainital 263002, India*

Accepted 2022 May 6. Received 2022 May 5; in original form 2022 April 3

ABSTRACT

We report observations of a bright dumb-bell system of galaxies ($z = 0.162$) with the upgraded Giant Metrewave Radio Telescope (*u*GMRT), which show that each member of this gravitationally bound pair of galaxies hosts bipolar radio jets extended on 100 kpc scales. Only two cases of such radio morphology have been reported previously, both being dumb-bell systems, as well. The famous first example, 3C 75, was discovered 4 decades ago, and the second case was discovered 3 decades ago. This implies that such 'Twin-Radio-Galaxies' (TRGs) are an exceedingly rare phenomenon. As in the case of its two senior cousins, the bipolar radio jets of the present TRG (J104454+354055) exhibit strong wiggles and are edge-darkened (Fanaroff–Riley class I). However, there are important differences, too. For instance, the jets in the present TRG do not merge and, moreover, show no signs of distortion due to an external crosswind. This makes the present TRG a much neater laboratory for studying the physics of (sideway) colliding jets of relativistic plasma. This TRG has a Wide-Angle-Tail neighbour hosted by another bright galaxy belonging to the same group, which appears to be moving towards the TRG.

Key words: galaxies: active – galaxies: jets.

1 INTRODUCTION

Galaxy mergers are the bedrock of the evolving cosmic structure leading to hierarchical galaxy formation (e.g. Barnes & Hernquist 1996; Bell et al. 2006). Since practically all large galaxies are believed to harbour a supermassive black hole (SMBH) (Magorrian et al. 1998; Richstone et al. 1998; Kormendy & Ho 2013), the possibility of SMBH coalescense due to galaxy mergers (e.g. Begelman, Blandford & Rees 1980; Gualandris et al. 2017, and references therein) has become a driver for the rapidly advancing new field of gravitational-wave astronomy (e.g. Hughes 2003; Amaro-Seoane et al. 2017; Jenkins 2022). From an observational viewpoint, if one or both members in the merging galaxy pair host a radio-loud active galactic nucleus (AGN), this can serve as a direct tracer of the SMBH merger process, via monitoring by Very Long Baseline Interferometry (VLBI). The prospects become much more exciting when *both* AGN are radio loud (Owen et al. 1985; Simpson & Rawlings 2002). The main techniques used to search for SMBH binaries (i.e. dual AGN) include photometric and spectroscopic measurements and radio interferometric imaging which is particularly promising because of the high resolution it can provide (e.g. Komossa et al. 2003; Liu et al. 2010; Bogdanović 2015; Shangguan et al. 2016; Rubinur et al. 2021). However, the success rate in finding merging SMBHs with discernible radio jets has been minuscule (e.g. Burke-Spolaor 2011; Tremblay et al. 2016), with just a few reasonably compelling cases reported so far.

On the smallest scale (<0.1 pc), the BL Lac object OJ 287 remains the only strong case for hosting an SMBH binary, as gleaned from its (paired) optical outbursts, recurring every ∼12 yr (Sillanpää et al. 1988). Its long-term optical light curve has been modelled in terms of an SMBH binary with an orbital semimajor axis of 0.05 pc, whose secondary crosses the accretion disc of the primary SMBH twice during each orbit (e.g. Lehto & Valtonen 1996; Valtonen et al. 2016; Dey et al. 2021; see also Britzen et al. 2018). Even on slightly larger (parsec) scale, only a couple of dual radio-AGN candidates seem genuine, the most prominent being the source 0402+379 for which VLBI has yielded an SMBH binary separation of ∼7 pc (Rodriguez et al. 2006; Burke-Spolaor 2011; Bansal et al. 2017). More recently, a dual radio-AGN, with an SMBH separation of just 0.35 pc has been found in the Seyfert galaxy NGC 7674 at $z = 0.0289$ (Kharb, Lal & Merritt 2017).

It is worth noting that while assessing the genuineness of such radio-loud cases, one needs to guard against the possibility that

★ E-mail: rvjoshirv@gmail.com

the candidate dual radio-AGN may turn out to be just (i) a pair of knots in a VLBI jet, or (ii) hot spots in a single compact-symmetric radio source (see e.g. Wrobel, Walker & Fu 2014), or (iii) even a case of (superluminal) gravitational milli-lensing (Gopal-Krishna & Subramanian 1996). Naturally, the binarity becomes much less ambiguous when the two radio nuclei are separated on kiloparsec scale (permitting detailed radio imaging), even though such SMBH pairs are clearly remote from an eventual merger. So far, just two cases of gravitationally bound pairs of radio galaxies with kiloparsec-scale jets have been identified, each hosted by a pair of similarly bright elliptical galaxies within a common envelope (dumb-bell). The famous first example of such 'Twin-Radio-Galaxy (TRG)' is the proto-type 3C 75, a Wide-Angle-Tail (WAT) radio source of overall size ∼0.5 Mpc, located near the centre of the galaxy cluster Abell 400 ($z = 0.023$). It was discovered almost 4 decades ago (Owen et al. 1985), which testifies to the extreme rarity of this cosmic phenomenon. The second TRG, which was discovered 3 decades ago and has received much less attention, is the source PKS 2149-158 of size ∼400 kpc, located near the outskirts of the cluster Abell 2382 ($z = 0.062$) (Parma, de Ruiter & Cameron 1991; Guidetti et al. 2008).

In this paper, we report the discovery of the third case of a bound pair of galaxies, each of which has a bipolar radio jet extended >100 kpc scale. The dumb-bell galaxy lies at the centre of a galaxy group at $z \sim 0.16$ (Yuan, Han & Wen 2016). This source was initially classified as an X-shaped radio galaxy candidate (Joshi et al. 2019; Yang et al. 2019), but in a follow-up programme with upgraded Giant Metrewave Radio Telescope (*u*GMRT), it was found to be a TRG. Here, we report radio-optical properties of this TRG and briefly compare it with the other two TRGs mentioned above. Throughout this paper, a cosmology with $H_0 = 70\,\mathrm{km\,s^{-1}\,Mpc^{-1}}$, $\Omega_\mathrm{m} = 0.3$, and $\Omega_\Lambda = 0.7$ is adopted. This gives a luminosity distance of 780 Mpc for the TRG and a scale of 2.797 kpc per arcsecond at the source redshift of $z = 0.16278$.

2 OBSERVATIONS AND ANALYSIS

The inset in Fig. 1(a) shows a *g*, *r*, *z* colour composite image from the Dark Energy Camera Legacy survey (DECaLS) (Dey et al. 2019) of the dumb-bell consisting of the galaxies 'A' & 'B', both with $z \simeq 0.162$, and a third, fainter galaxy 'C' of unknown redshift, within the same stellar halo. The colour composite image of another bright galaxy 'D', which has a redshift of 0.160 and is located 2.72 arcmin (= 456 kpc) west of the dumb-bell is shown in the inset of Fig. 1(c). Particulars of these four galaxies are given in Table 1. Low-resolution optical spectroscopic observations of the dumb-bell system were carried out using the HFOSC instrument mounted on the 2m-Himalayan Chandra Telescope (Prabhu 2014), with grisms Gr#7 (3500–7800 Å) and slit-width of 2.0 arcsec. The data were reduced with the standard IRAF[1] package. The optical spectra were modelled using the penalized PiXel-Fitting method (pPXF, Cappellari & Emsellem 2004; Cappellari 2017) and the measured stellar velocity dispersions of $\sigma_* = 412.2 \pm 34.8$ km s^{-1} and 254.5 ± 20.4 km s^{-1} for the galaxies A and B were used to estimate the black hole masses (Greene, Strader & Ho 2020, see their table 5) (see Table 1). The non-detection of [O III]λ5007Å nebular emission line for both galaxies implies that they are low-excitation radio galaxies (LERGs) (Best & Heckman 2012).

The radio observations were made using the *u*GMRT, in the band-5 (900 to 1450 MHz), with 400 MHz bandwidth encompassing 2048 channels (Swarup et al. 1991; Gupta et al. 2017). The data were reduced following the standard procedures, using the Astronomical Image Processing System (AIPS).[2] While calibrating the data, bad data were flagged out at various stages. The data for antennas with large errors in antenna-based solutions were checked and flagged over the requisite time ranges. The flux calibration was performed using 3C 286 and the flux density scale defined by Perley & Butler (2013). The phase calibration was done using the source 1033+395.[3] The final image was made after several rounds of phase self-calibration, and one round of amplitude self-calibration. An on-source time of 48 min resulted in an rms noise of 34 μJy beam^{-1}, where the beamsize is 3.15 arcsec × 1.73 arcsec (PA = 71 deg) (Fig. 1).

3 RESULTS

In the uGMRT map, both members of the dumb-bell system, namely A and B (Table 1), are seen to eject wiggling bipolar radio jets along roughly the same direction (Fig. 1). Both northern jets are brighter than their southern counterparts and, after maintaining a steady mutual separation over the initial ∼30 kpc (projected), the two northern jets become diffuse but do not appear to merge (see Section 4). The (fainter) two jets on the southern side remain separated all along, despite strong wiggling. The observed projected extents of the bipolar jets associated with A and B are ∼220 and ∼140 kpc, respectively (Fig. 1). The 144 MHz radio maps from the LOFAR Two-meter Sky Survey Data Release 2 (LoTSS-DR2) (Shimwell et al. 2022) have revealed more extended, bright radio emission connected to the southern jets, whereas a faint, long radio spur of size ∼60 arcsec is detected on the northern side (Fig. 1). Thus, the source has an overall size of at least 3.0 arcmin (i.e. 0.5 Mpc). However, the TRG morphology is not discernible in the LoTSS map, due to its relatively large beam size of 6 × 6 arcsec (see Fig. 1). Consistent with their moderate radio luminosities (Table 1), both radio galaxies exhibit an edge-darkened (Fanaroff–Riley class I) morphology (Fanaroff & Riley 1974; Ledlow & Owen 1996). Fig. 2 shows the integrated radio spectrum ($S_\nu \propto \nu^\alpha$, where ν and S_ν are the frequency and flux density, respectively), of this dumb-bell system (A + B), which is consistent with a straight line of spectral index $\alpha = -0.74$. For the radio cores of the galaxies A and B, the VLASS maps (Lacy et al. 2020) give flux densities of 5.6 ± 0.3 and 2.8 ± 0.3 mJy at 3 GHz, respectively. The galaxy C remained undetected in both VLASS and the present uGMRT observations, setting an upper limit of 1.4 mJy at 1.4 GHz. The *u*GMRT map of the source D (Fig. 1) shows its radio jets emerging at PA ≈ 70 deg, although after ∼20 arcsec (≃56 kpc) the eastern jet undergoes a sharp bending towards the north-west, giving the source a 'WAT' morphology (see Owen & Rudnick 1976; Jones & Owen 1979). From the VLASS, its core is found to have a flux density of 1.1 ± 0.2 mJy at 3 GHz. Its integrated radio spectral index is −0.75, based on the NVSS flux density of 23.4 ± 1.3 mJy at 1.4 GHz (Condon et al. 1998) and LoTSS-DR2 flux density of 127.7 ± 12.2 mJy at 144 MHz (Shimwell et al. 2022).

[1] IRAF is distributed by the National Optical Astronomy Observatories, which are operated by the Association of Universities for Research in Astronomy, Inc., under cooperative agreement with the National Science Foundation.

[2] http://www.aips.nrao.edu

[3] http://www.vla.nrao.edu/astro/calib/manual/csource.html

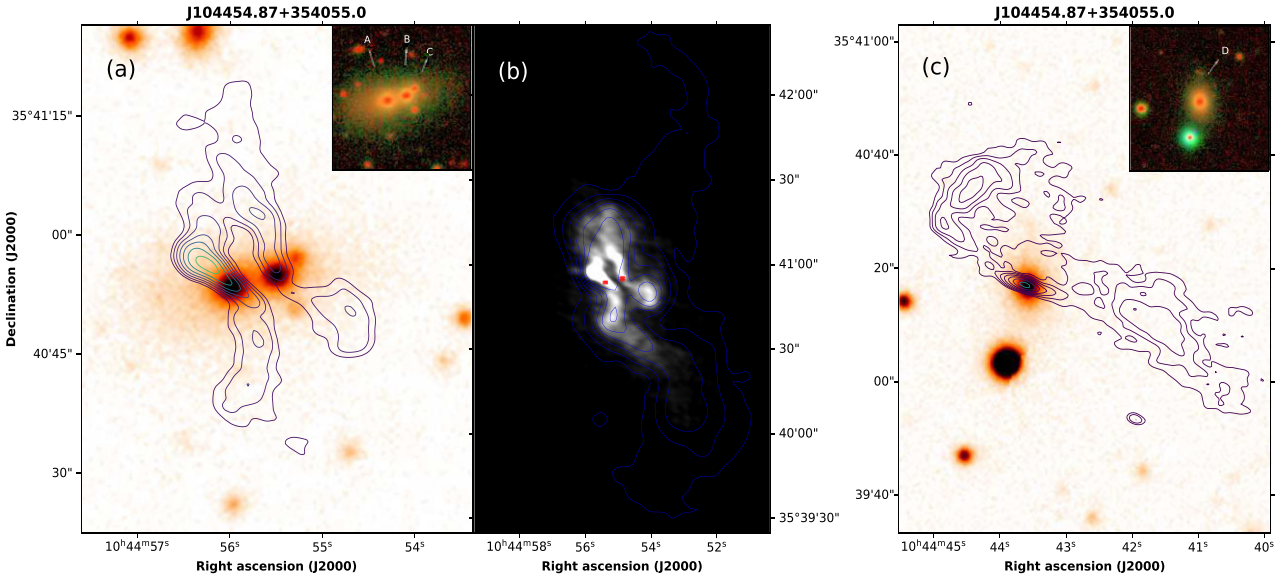

Figure 1. *Left-hand panel:* The radio-optical overlay shows the *u*GMRT 1.4 GHz radio contours overlaid on to the *r*-band image from the DECaLS (Dey et al. 2019) of the dumb-bell galaxy pair 'A' and 'B'. The inset shows the *g*-, *r*-, *z*-band colour-composite image from the DECaLS of the dumb-bell galaxy pair together with an apparently close radio-quiet galaxy 'C'. *Middle panel* shows the grey-scale uGMRT image of the pair of bipolar jets (TRG) overlaid with the 144 MHz LoTSS-DR2 radio contours. The positions of the respective host galaxies are marked with red dots. *Right-hand panel:* Radio-optical overlay of the *u*GMRT 1.4 GHz radio contours of the 'WAT' radio galaxy 'D' whose *g*-, *r*-, *z*-band colour-composite DECaLS image is shown within the inset. Contours levels are set at square-root increment of (2, 4, 8, 16, 32,...) × 14σ for the TRG and × 5σ for the WAT source, where σ rms noise is 34 μJy beam^{-1} for the our uGMRT maps. The LoTSS counter levels are set at (1, 16, 81, 256,...) × 3σ, where σ rms noise is 87 μJy beam^{-1}.

Table 1. Basic parameters of the four galaxies based on optical and radio *u*GMRT observations.

Source	RA (J2000)	Dec. (J2000)	Redshift * z	log M_{BH} $M_\odot$	Type	Flux density (mJy) Core†	North-jet	South-jet	Length (arcsec) North-jet	South-jet	Total	Radio luminosity log(L_R) (erg s^{-1})
A	$10^h44^m55\overset{s}{.}36$	$+35°40'53\overset{''}{.}5$	0.16173	10.2 ± 0.4	LERG	5.6 ± 0.3	21.8	40.8	29.7	51.3	78.9	42.43
B	$10^h44^m54\overset{s}{.}87$	$+35°40'55\overset{''}{.}0$	0.16278	9.3 ± 0.3	LERG	2.8 ± 0.3	36.1	23.5	31.7	20.0	51.3	42.36
C	$10^h44^m54\overset{s}{.}67$	$+35°40'57\overset{''}{.}1$	–	–	–	≤1.4 (5σ)	–	–	–	–	–	–
						Core	West-jet	East-jet	West-jet	East-jet	Total	
D	$10^h44^m41\overset{s}{.}85$	$+35°40'16\overset{''}{.}7$	0.16007	9.4 ± 0.2	LERG	1.1 ± 0.2	19.5	20.4	46.6	26.1	73.8	41.87

Notes. †The core flux densities are estimated using the VLASS radio map at 2.5 GHz (Lacy et al. 2020). The other radio parameters are derived from 1.4 GHz uGMRT maps (this work).
*The redshift of the galaxies B and D are taken from the SDSS archive (Ahumada et al. 2020).

4 DISCUSSION

Indubitably, a key message from this study is that TRGs, each having a kiloparsec-scale bipolar radio jet, are an extremely rare phenomenon. The source J104454+354055 reported here becomes the third known TRG, the first one (3C 75) was reported 37 yr ago and the second one (PKS 2149-158) 31 yr ago. All three TRGs are associated with dumb-bell systems residing in galaxy clusters/groups (Section 1). A prognosis of their extreme rarity came long ago from a VLA survey of 88 compact groups of galaxies (Menon & Hickson 1985). These authors concluded that any bright radio emission arising from a galaxy group is usually associated with its brightest member galaxy, while the remaining group members are radio-quiet. They found a strong preference for the radio-loud elliptical galaxy in a group to be the first-ranked; even relatively luminous ellipticals holding second or third rank were found to be radio-quiet. A robust theoretical underpinning to this empirical result still remains elusive.

Several parallels can be drawn between the present TRG and its two senior cousins, namely the famous and extensively studied 3C 75 and the TRG PKS 2149-158 (Section 1). As mentioned above, the galaxy pairs hosting all these three TRGs reside in a group/cluster environment, a circumstance clearly more conducive to the formation of dumb-bell systems. Secondly, all three TRGs exhibit FR I morphology, consistent with their moderate radio luminosities. Their radio jets, imaged at 1.4 GHz with a similar resolution of ∼5 arcsec, too are similarly extended on 100 kpc scales. Also, the apparent separation between their twin host galaxies is around 10 kpc (between 8 and 18 kpc) and the line-of-sight velocity difference between the paired host galaxies are quite similar: ∼ 430 km s^{-1} (3C 75) (Lauer et al. 2014), ∼ 546 km s^{-1} (PKS 2149-158) (Owen, Ledlow & Keel 1995; Smith et al. 2004), and ∼ 300 km s^{-1} (present TRG) (see Table 1). However, beyond these basic similarities, salient differences are noticeable between the three TRGs. Next, we enumerate some of these contrasts, as they might hold vital clues from the perspective of theoretical modelling and numerical simulations, especially once the other two TRGs have been observed in detail comparable to the proto-type 3C 75.

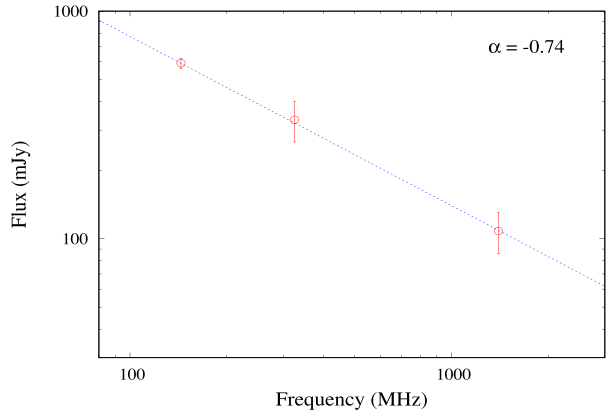

Figure 2. Integrated radio spectrum of the present TRG J1044+3540, using the flux densities from the 144 MHz LoTSS-DR2 (Shimwell et al. 2022), 325 MHz WENSS (Rengelink et al. 1997), and NVSS 1.4 GHz (Condon et al. 1998). The beamsize for the latter two maps is around 0.75–0.9 arcmin. Therefore, the LoTSS-DR2 map was smoothed to a beamwidth of 0.8 arcmin. The measured intergrated flux densities at the three frequencies are: 590 ± 31 mJy (144 MHz), 333 ± 67 mJy (325 MHz), and 108 ± 22 mJy (1.4 GHz).

(i) While all three TRGs exhibit conspicuously wiggly jets, the two northern jets of 3C 75 are seen to merge into a single entity, fairly early on [a similar situation probably exists in the other TRG, PKS 2149-158, although even its best available (VLA) map lacks sufficient clarity, see Guidetti et al. 2008]. This contrasts with the present TRG in which both bipolar jets retain their distinct identities much farther out, providing a greater space for their kinematical modelling.

(ii) In 3C 75, situated at the centre of the cluster Abell 400, all four jets undergo a sharp bending towards east/north-east (Owen et al. 1985). This is attributed to dynamic pressure exerted by an intra-cluster crosswind blowing at a speed of ∼1200 km s^{-1} (Hudson et al. 2006), due to the ongoing merger of the host cluster Abell 400 with a subcluster (e.g. Beers et al. 1992; Hudson et al. 2006). This extraneous factor poses a complication to analytical modelling and numerical simulations of the basic phenomenon of twin bipolar jets (e.g. Molnar et al. 2017; Musoke et al. 2020, see also, Steinborn et al. 2016). A similar structural complexity appears to plague the twin bipolar jets of the second TRG PKS 2149-158, which exhibit a conspicuous C-shaped bending (Guidetti et al. 2008), again indicating a strong dynamical pressure acting on the jets. In contrast, the present TRG is a much neater system, as the impact of the orbital motion of the two galaxies A and B on the morphologies of their bipolar jets is not contaminated by ram-pressure of a cross-wind. This would simplify the dynamical modelling of the twin bipolar jets, since there is no need to disentangle the effect of the orbital motion of the host galaxy pair from extraneous forces due to cross-wind impinging on the jets. To appreciate this point, we may recall that the orbital motion of the paired host galaxies is expected to impose a mirror-symmetric wiggling on the bipolar jet pair, as is indeed observed in the uGMRT image of the present system and which also lends further support to the assertion that the two bipolar jets are physically associated (Fig. 1). In the other two TRGs, the wiggly pattern of jets is massively distorted due to the dynamical impact of the intracluster cross-wind, as mentioned above. The inference then is that the present TRG is a superior laboratory for probing the physics of two nearly parallel wiggly jets of relativistic plasma bouncing sideways against each other, but escaping disruption (Fig. 1). Also, all four jets of the present TRG are bright enough for radio polarimetry, which would enable mapping of their magnetic field and investigating its possible role in preserving the identity of the relativistic plasma jets bouncing against each other.

4.1 The WAT neighbour

As mentioned in Section 3, the *u*GMRT map also shows a WAT radio galaxy (D), located 2.72 arcmin (= 456 kpc) to the west of the present TRG (Fig. 1c). The twin-jets of the WAT initially advance along PA ∼ 70 deg, for ∼60 kpc, when the eastern jet undergoes a sharp bend towards north-west. Plausibly, the strong dynamic pressure required for the jet bending comes from motion of the host galaxy towards the dumb-bell system and its associated gaseous halo. In order to assess such a possibility, we estimate the zone of gravitational influence of the dumb-bell, i.e. its virial radius, which is roughly the range out to which the gaseous halo of the dumb-bell system might extend.

Using the 2MASS *K*-band apparent magnitudes of the dumb-bell constituents A and B, of $K = 14.48$, and 14.89, respectively, we estimate their absolute magnitudes (M_K) taking a distance modulus of 39.4 and K-corrections of −0.27 and −0.28 (Chilingarian, Melchior & Zolotukhin 2010; Chilingarian & Zolotukhin 2012). This yields $M_K = -25.1$ and −24.77 for A and B, respectively. These correspond to stellar masses of $\log M_* \sim 11.50\,M_\odot$ and $11.35\,M_\odot$ for A and B (Cappellari 2013, equation 2), amounting to a total stellar mass of $\log M_* \sim 11.73 M_\odot$ for the galaxy pair. Galaxy stellar-to-halo mass relation (SHMR) implies their dark halo virial masses to be $\log M_{\rm vir} \sim 14.1 M_\odot$ and $\sim 13.8 M_\odot$, respectively (Moster et al. 2010, equation 2; Wechsler & Tinker 2018). Such massive haloes are typically assembled by a redshift of $z_a \sim 0.8$, and have virial radii given by Shull (2014):

$$\frac{R_{\rm vir}}{206\ {\rm kpc}} \approx \left(\frac{M_{\rm vir}}{10^{12} M_\odot}\right)^{1/3} (1+z_a)^{-1} \qquad (1)$$

For the total mass of the dumb-bell system ($\log M_{\rm vir} \sim 14.3 M_\odot$), its virial radius is then expected to extend to ∼670 kpc, i.e. beyond the galaxy D identified with the WAT and is thus available for exerting the dynamic pressure required for the observed bending of its jet (Fig. 1c).

5 CONCLUSIONS

The *u*GMRT observations reported here have revealed of a pair of bipolar extended radio jets emanating from a dumb-bell system containing two gravitationally bound massive elliptical galaxies within a common stellar envelope. This newly discovered 'TRG', J104454+354055, is the third TRG found so far. The first (famous) example of this extremely rare class, the TRG 3C 75, was discovered 37 yr ago, followed by the discovery of a second (much less known) TRG PKS 2149-158 3 decades ago. All four jets of the present TRG are extended on 100-kpc scale and exhibit an edge-darkened radio morphology (FR I), as well as a mirror-symmetric wiggly pattern which is consistent with both host galaxies performing orbital motion about a common gravitational centre (the recent LoTSS/DR2 map shows a total size of ∼0.5 Mpc). Unlike the other two TRGs, there is no indication that the jets of the present TRG merge with each other early on, or become distorted due to a cross-wind. This goes to make this TRG a much neater exponent of cosmic tango, more amenable to modelling the jet dynamics in TRGs and for studying the impact of sideway collisions of relativistic plasma jets on their survivability (e.g. Achterberg 1988; Musoke et al. 2020). A third bright radio galaxy in this group is found to be a WAT apparently in motion directed towards the dumb-bell system. Radio spectral and

polarimetric imaging of the present TRG, supplemented with X-ray observations yielding gas pressures within the group, and numerical simulations, would be very desirable for a deeper understanding of the evolution of closely interacting synchrotron jets.

ACKNOWLEDGEMENTS

GK acknowledges a Senior Scientist fellowship of the Indian National Science Academy (INSA). DP acknowledges the post-doctoral fellowship of the S. N. Bose National Centre for Basic Sciences, Kolkata, India, funded by the Department of Science and Technology (DST), India. XLY thanks the National Science Foundation of China (12103076), the Shanghai Sailing Program (21YF1455300), and the China Postdoctoral Science Foundation (2021M693267) for support, LCH was supported by the National Science Foundation of China (11721303, 11991052, 12011540375) and the China Manned Space Project (CMS-CSST-2021-A04). This research has used the 'K-corrections calculator' service available at http://kcor.sai.msu.ru/. We thank the staff of the GMRT that made these observations possible. GMRT is run by the National Centre for Radio Astrophysics of the Tata Institute of Fundamental Research. We thank the staff of IAO, Hanle and CREST, Hosakote, that made these observations possible. The facilities at IAO and CREST are operated by the Indian Institute of Astrophysics, Bangalore.

DATA AVAILABILITY

The radio data used in this study will be publicly available at *u*GMRT data archive at https://naps.ncra.tifr.res.in/goa/data/search

REFERENCES

Achterberg A., 1988, A&A, 191, 167
Ahumada R. et al., 2020, ApJS, 249, 3
Amaro-Seoane P. et al., 2017, preprint (arXiv:1702.00786)
Bansal K., Taylor G. B., Peck A. B., Zavala R. T., Romani R. W., 2017, ApJ, 843, 14
Barnes J. E., Hernquist L., 1996, ApJ, 471, 115
Beers T. C., Gebhardt K., Huchra J. P., Forman W., Jones C., Bothun G. D., 1992, ApJ, 400, 410
Begelman M. C., Blandford R. D., Rees M. J., 1980, Nature, 287, 307
Bell E. F., Phleps S., Somerville R. S., Wolf C., Borch A., Meisenheimer K., 2006, ApJ, 652, 270
Best P. N., Heckman T. M., 2012, MNRAS, 421, 1569
Bogdanović T., 2015, in Gravitational Wave Astrophysics, p. 103
Britzen S. et al., 2018, MNRAS, 478, 3199
Burke-Spolaor S., 2011, MNRAS, 410, 2113
Cappellari M., 2013, ApJ, 778, L2
Cappellari M., 2017, MNRAS, 466, 798
Cappellari M., Emsellem E., 2004, PASP, 116, 138
Chilingarian I. V., Melchior A.-L., Zolotukhin I. Y., 2010, MNRAS, 405, 1409
Chilingarian I. V., Zolotukhin I. Y., 2012, MNRAS, 419, 1727
Condon J. J., Cotton W. D., Greisen E. W., Yin Q. F., Perley R. A., Taylor G. B., Broderick J. J., 1998, AJ, 115, 1693
Dey A. et al., 2019, AJ, 157, 168
Dey L., Valtonen M. J., Gopakumar A., Lico R., Gómez J. L., Susobhanan A., Komossa S., Pihajoki P., 2021, MNRAS, 503, 4400
Fanaroff B. L., Riley J. M., 1974, MNRAS, 167, 31P
Gopal-Krishna, Subramanian K., 1996, A&A, 315, 343
Greene J. E., Strader J., Ho L. C., 2020, ARA&A, 58, 257
Gualandris A., Read J. I., Dehnen W., Bortolas E., 2017, MNRAS, 464, 2301
Guidetti D., Murgia M., Govoni F., Parma P., Gregorini L., de Ruiter H. R., Cameron R. A., Fanti R., 2008, A&A, 483, 699
Gupta Y. et al., 2017, Curr. Sci., 113, 707
Hudson D. S., Reiprich T. H., Clarke T. E., Sarazin C. L., 2006, A&A, 453, 433
Hughes S. A., 2003, Ann. Phys., 303, 142
Jenkins A. C., 2022, preprint (arXiv:2202.05105)
Jones T. W., Owen F. N., 1979, ApJ, 234, 818
Joshi R. et al., 2019, ApJ, 887, 266
Kharb P., Lal D. V., Merritt D., 2017, Nat. Astron., 1, 727
Komossa S., Burwitz V., Hasinger G., Predehl P., Kaastra J. S., Ikebe Y., 2003, ApJ, 582, L15
Kormendy J., Ho L. C., 2013, ARA&A, 51, 511
Lacy M. et al., 2020, PASP, 132, 035001
Lauer T. R., Postman M., Strauss M. A., Graves G. J., Chisari N. E., 2014, ApJ, 797, 82
Ledlow M. J., Owen F. N., 1996, AJ, 112, 9
Lehto H. J., Valtonen M. J., 1996, ApJ, 460, 207
Liu X., Greene J. E., Shen Y., Strauss M. A., 2010, ApJ, 715, L30
Magorrian J. et al., 1998, AJ, 115, 2285
Menon T. K., Hickson P., 1985, ApJ, 296, 60
Molnar S. M., Schive H. Y., Birkinshaw M., Chiueh T., Musoke G., Young A. J., 2017, ApJ, 835, 57
Moster B. P., Somerville R. S., Maulbetsch C., van den Bosch F. C., Macciò A. V., Naab T., Oser L., 2010, ApJ, 710, 903
Musoke G., Young A. J., Molnar S. M., Birkinshaw M., 2020, MNRAS, 494, 5207
Owen F. N., Ledlow M. J., Keel W. C., 1995, AJ, 109, 14
Owen F. N., O'Dea C. P., Inoue M., Eilek J. A., 1985, ApJ, 294, L85
Owen F. N., Rudnick L., 1976, ApJ, 205, L1
Parma P., de Ruiter H. R., Cameron R. A., 1991, AJ, 102, 1960
Perley R. A., Butler B. J., 2013, ApJS, 204, 19
Prabhu T. P., 2014, Proc. Indian Natl. Sci. Acad. A, 80, 887
Rengelink R. B., Tang Y., de Bruyn A. G., Miley G. K., Bremer M. N., Roettgering H. J. A., Bremer M. A. R., 1997, A&AS, 124, 259
Richstone D. et al., 1998, Nature, 395, A14
Rodriguez C., Taylor G. B., Zavala R. T., Peck A. B., Pollack L. K., Romani R. W., 2006, ApJ, 646, 49
Rubinur K., Kharb P., Das M., Rahna P. T., Honey M., Paswan A., Vaddi S., Murthy J., 2021, MNRAS, 500, 3908
Shangguan J., Liu X., Ho L. C., Shen Y., Peng C. Y., Greene J. E., Strauss M. A., 2016, ApJ, 823, 50
Shimwell T. W. et al., 2022, A&A, 659, A1
Shull J. M., 2014, ApJ, 784, 142
Sillanpää A., Haarala S., Valtonen M. J., Sundelius B., Byrd G. G., 1988, ApJ, 325, 628
Simpson C., Rawlings S., 2002, MNRAS, 334, 511
Smith R. J. et al., 2004, AJ, 128, 1558
Steinborn L. K., Dolag K., Comerford J. M., Hirschmann M., Remus R.-S., Teklu A. F., 2016, MNRAS, 458, 1013
Swarup G., Ananthakrishnan S., Kapahi V. K., Rao A. P., Subrahmanya C. R., Kulkarni V. K., 1991, Curr. Sci., 60, 95
Tremblay S. E., Taylor G. B., Ortiz A. A., Tremblay C. D., Helmboldt J. F., Romani R. W., 2016, MNRAS, 459, 820
Valtonen M. J. et al., 2016, ApJ, 819, L37
Wechsler R. H., Tinker J. L., 2018, ARA&A, 56, 435
Wrobel J. M., Walker R. C., Fu H., 2014, ApJ, 792, L8
Yang X. et al., 2019, ApJS, 245, 17
Yuan Z. S., Han J. L., Wen Z. L., 2016, MNRAS, 460, 3669

This paper has been typeset from a TEX/LATEX file prepared by the author.